Journal of Hazardous Materials, 16 (1987) 149–172
Elsevier Science Publishers B.V., Amsterdam — Printed in The Netherlands

A STATISTICAL EXAMINATION OF WIND TUNNEL MODELLING OF THE THORNEY ISLAND TRIALS

M.E. DAVIES and P.N. INMAN

British Maritime Technology Ltd., Teddington, Middlesex (Great Britain)

(Received October 31, 1986; accepted February 20, 1987)

Summary

A large number of wind tunnel simulations of Thorney Island heavy gas trials have been performed to establish overall trends with model scale and source condition. Most of the analysis has been based on the comparison of peak concentrations at model and full scale. Within the confidence of determining trends from such a set of results support is given to the validity of relatively small scale modelling, particularly in the presence of sharp edged dispersing elements such as fences.

1. Introduction

During 1982–1984 the heavy gas dispersion trials at Thorney Island produced a large data base of concentration measurements in a variety of circumstances. Phases I and II have been well reported [1,2] and Phase III covered additional ground on vapour fences for the U.S. Coast Guard and Dept. of Transportation. In Phase III the 2.4 m vapour fence enclosed the original gas release container (used as a reservoir) and the ground level continuous release vent. The enclosure was rectangular with dimensions 54 m by 26 m. The series contained, in all, around 40 "good" gas spills and with typically 250 channels available for data recording, a considerable challenge has been placed on analysts to derive full benefit. Many of the studies are reported elsewhere in this volume and their range demonstrates the different approaches to the data that can be taken. They cover overall principles (variability and fundamental physical processes), general descriptions (cloud properties, mass flux balances, meteorological and atmospheric turbulence data) and specific and general modelling validation exercises. The work described in this paper falls in the last category and is an attempt to express an overall statement of confidence in the applicability of wind tunnel modelling to these types of heavy gas release. The approach has been to generate the same statistics for a large number of model–full scale comparisons and to examine the overall trends, thereby reduc-

0304-3894/87/$03.50

ing the impact of variability (model or full scale) and any residual uncertainty in the trials or model data.

The aim was to undertake enough simulations at enough typical model scales, to allow broad comparison data to be presented, as a guide to the prediction of hazards using such tools and to point out particular types of phenomena which are markedly more or less well simulated.

2. Modelling programme

Model scales from 1:40 to 1:250 were employed in simulating Thorney Island trials. The range was intended to span scales likely to be used in hazard prediction studies and the choices were not, therefore, optimised in any way for this study. A 1:250 scale should in fact be recognized as a particularly small scale in view of the small "full scale" dimensions of the Thorney Island set-up. To illustrate the point Fig. 1 shows where the 2.4 m vapour fence in Phase III would stand in the smooth wall wind-tunnel turbulent boundary layers with Froude scaled velocities.

The undisturbed cloud depth in the vapour enclosure would be around 1.5 m and although Fig. 1 does not represent the disturbed flow field due to the fence

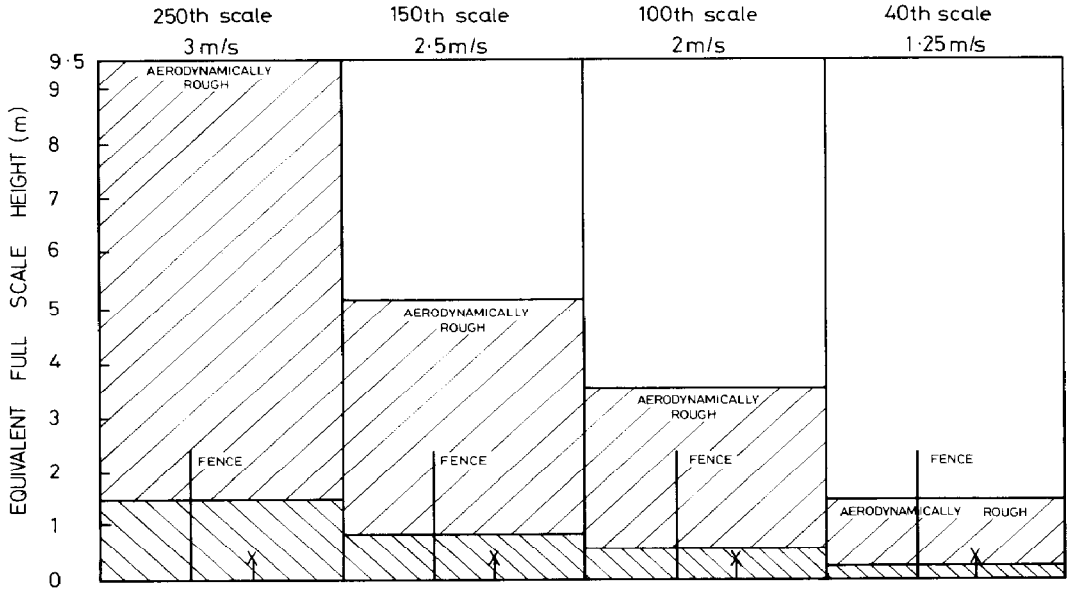

Fig. 1. Wind tunnel boundary layer on a smooth surface at the lowest operational speed (~ 0.2 m/s at an equivalent height to 10 m full scale). Smooth-wall boundary layer: ▨ viscous sub-layer $0 < z_+ < 5$, ▨ buffer layer $5 < z_+ < 30$, log law $z_+ > 30$, where $z_+ = zu^*/\nu$. Characteristic length scale of uniformly distributed roughness elements to create a fully aerodynamically rough surface: $z_+ > 30$. × = Lowest gas sensor.

and gas container, it is nonetheless reasonable to suppose that viscous effects might be strong at the smallest scales. To generalise these conclusions, of course, the scale factors need to be expressed in some non-dimensional form to compare with simulations of larger more "usual" hazard situations and this will be returned to in Section 4.

An extensive programme of wind tunnel tests was conducted and these are shown in Table 1. A number of different "Types" of dispersion experiment were performed at Thorney Island and these have been denoted in the table as:

1 – Instantaneous release in unobstructed flat terrain (Phase I)
2 – Instantaneous release in the presence of various obstructions (wall, porous fence, building) (Phase II)
3 – Continuous release in unobstructed flat terrain (Phases I and III)

TABLE 1

Schedule of wind tunnel simulations of Thorney Island heavy gas dispersion trials

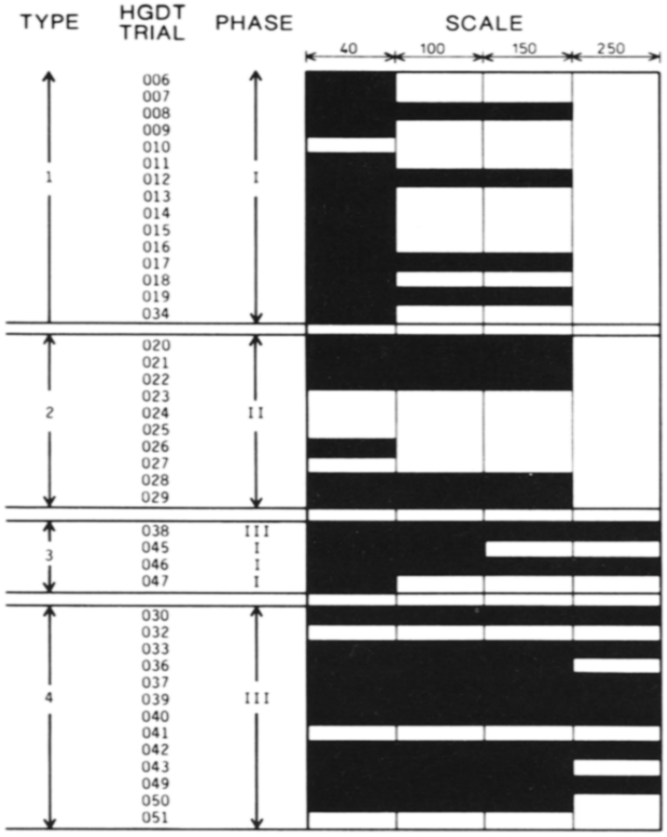

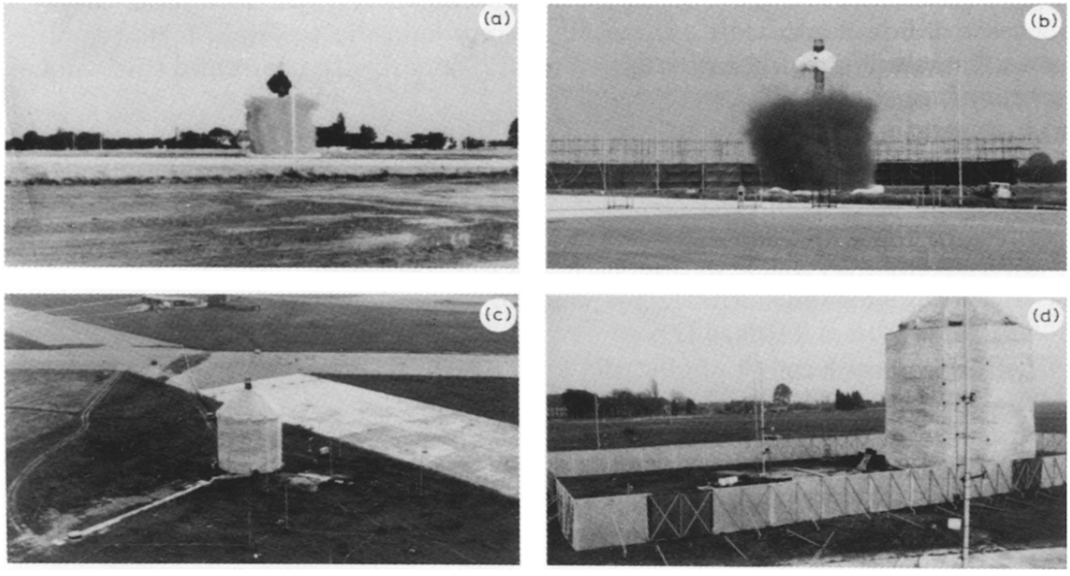

Fig. 2. Sample Thorney Island trials: (a) Type 1, (b) Type 2, (c) Type 3, and (d) Type 4.

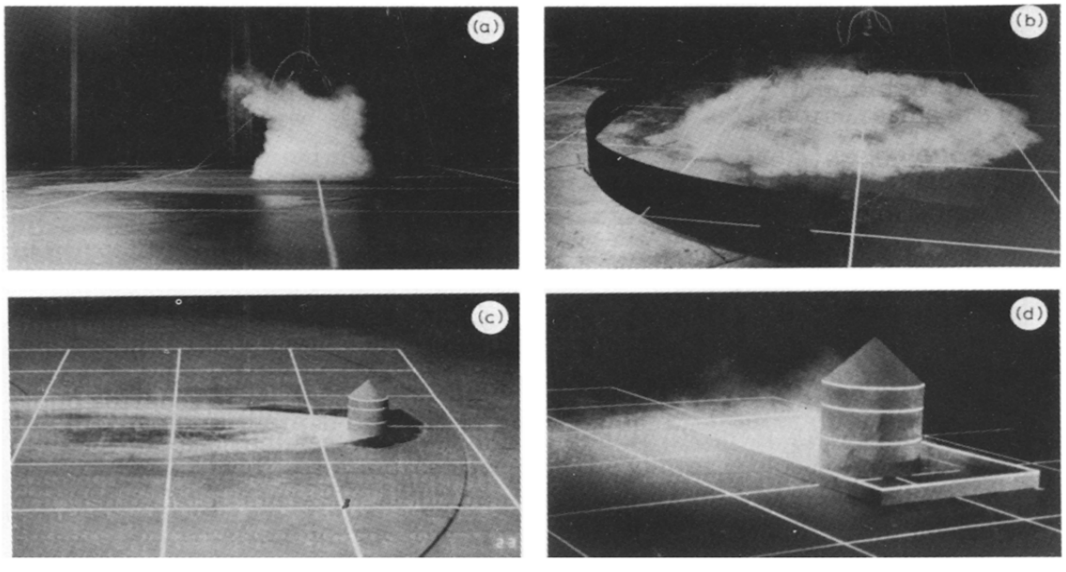

Fig. 3. Sample wind tunnel simulations: (a) Type 1, (b) Type 2, (c) Type 3, and (d) Type 4.

TABLE 2

Initial conditions for simulated spills

Trial no.	Phase/Type	Density ratio	U_{10} m/s	Volume m^3	Rate m^3/min	Bulk Richardson no.	Pasquill stability class
006	I/1	1.6	2.6	1580	—	8.9	D/E
007	I/1	1.8	3.2	2000	—	9.3	E
008	I/1	1.7	2.4	2000	—	15.5	D
009	I/1	1.6	1.7	2000	—	26.5	F
010	I/1	1.8	2.4	2000	—	17.7	C
011	I/1	2.0	5.1	2100	—	4.9	D
012	I/1	2.3	2.6	1950	—	24.7	E
013	I/1	2.0	7.5	1950	—	2.2	D
014	I/1	1.8	6.8	2000	—	2.1	C/D
015	I/1	1.4	5.4	2100	—	1.9	C/D
016	I/1	1.7	4.8	1580	—	3.0	D
017	I/1	4.2	5.3	1700	—	12.5	D/E
018	I/1	1.9	7.4	1700	—	1.7	D
019	I/1	2.1	6.6	2100	—	3.5	D/E
020	II/2	1.9	5.6	1920	—	3.5	C/D
021	II/2	2.0	3.9	2050	—	9.0	D/E
022	II/2	4.2	6.0	1400	—	7.8	D/E
026	II/2	2.0	1.9	1970	—	35.0	B
028	II/2	2.0	9.0	1850	—	1.5	D
029	II/2	2.0	5.5	1950	—	4.1	D
030	III/4	1.4	4.3	1603	260	0.2	E
033	III/4	1.6	2.8	1870	340	1.2	D/E
034	I/1	1.8	1.4	2110	—	60.4	F
036	III/4	1.6	2.4	1963	310	1.6	F/G
037	III/4	1.6	3.2	1891	255	0.7	E
038	III/3	1.6	3.8	1867	280	0.5	F
039	III/4	1.4	5.8	1808	350	0.1	D
040	III/4	1.2	3.1	1860	310	0.2	D
042	III/4	1.6	3.4	1973	185	0.5	D
043	III/4	1.3	1.5	1899	265	2.5	F
045	I/3	2.0	2.3	1972	260	2.6	E/F
046	I/3	2.0	3.3	1490	260	1.0	D
047	I/3	2.0	1.5	1938	250	7.9	F
049	III/4	1.6	2.5	1907	260	1.3	F
050	III/4	1.4	1.74	1800	270	2.1	F

Bulk Richardson no. $= \frac{g\Delta\rho}{\rho}\frac{H}{U_{10}^2}$; H = initial cloud height (Instantaneous)

$= \frac{g\Delta\rho}{\rho}\frac{L}{U_{10}^2}$; $L = (Q/U_{10})^{\frac{1}{2}}$ (Continuous)

4 – Continuous release in a fenced enclosure (Phase III)

Sample photographs to illustrate these types are shown in Fig. 2 (full scale) and Fig. 3 (wind tunnel). As shown in Table 1, scales ranging from 1:40 to 1:250 were covered in simulating 34 of the trials. The particular scales chosen for each trial are shown in the bar chart and in total 86 simulations were performed. Typically 10 repeat wind tunnel runs each with up to 12 concentration probes were required to map the concentration field for each simulation and to produce point by point comparisons with the 10 to 20 "ground level" (0.4 m high) sensors which sensed gas in the trials. Details of the main parameters – initial density ratio, volume released/release rate, wind speed, atmospheric stability and bulk Richardson number, are given in Table 2. The main parametric variations were confined to wind speed and initial density ratio.

The experiments were performed in BMT's No. 7 boundary layer wind tunnel which has a working section 4.8 m wide, 2.4 m high and 15 m long. The facility is not capable of modelling atmospheric temperature gradients, so for these simulations the emphasis was placed on producing a suitable velocity and turbulence intensity profile for the Thorney Island site. In practice the full scale profiles were far from "classic" in shape [3] resulting, as they frequently did, from the complex boundary layer physics encountered at the end of a day of sea breezes, when rapid cooling and changing wind speed were prevailing.

For the purpose of assessing scale effects it seemed sensible, for this study, to preserve the fundamental parameters of density difference and Froude number $(\rho_g - \rho_a)/\rho_a$ and (gL/U^2). Clearly the Reynolds number (UL/ν) and Peclet number (UL/D) were small as a result and frequently the wind tunnel was operating at its lowest extreme (around 0.2 m/s). That this was a severe test of wind tunnel modelling capability was, however, part of the rationale of these tests. In practice, of the 86 simulations in Table 1, seven needed some modified Froude scaling* to be modelled at all. A minimum density increase was chosen and these values are shown in Table 3.

In the wind tunnel, Freon 12 and Argon mixtures provided the simulant heavy gas and concentration measurements were made with specially developed low-volume-flow aspirating probes (8 ml/s in air). The effective diameter of the ingested stream tube (deduced from continuity) is 6 mm in a 0.25 m/s stream. The equivalent diameter at full-scale varies from 0.24 m to 1.5 m depending upon the simulation scale. These figures give a guide to the possibility of direct probe interference when positioning probes in close proximity to one another, and indicate the effective spatial resolution of individual probes. The resulting averaging times are shown in Table 4. Additional timescale corrections were applied to the densimetric Froude scaled spills and in analyses where cross-scale comparisons have been made consistently averaged data has

*Modelling on the basis of densimetric Froude number, $g\Delta\rho L/\rho U^2$.

TABLE 3

Modified Froude scaled simulations

Spill no.	Scale	Density ratio (full scale)	Density ratio (model scale)
33	250	1.63	2.5
36	150	1.60	2.0
43	100	1.33	2.0
43	150	1.33	2.0
49	250	1.6	2.5
50	100	1.4	2.0
50	150	1.4	2.0

TABLE 4

Full scale equivalent averaging times for concentration probe

	Simulation scale				
	Full scale	1:40	1:100	1:150	1:250
Frequency response of probe (Hz)	1	10	10	10	10
Data sampling rate (Hz)	20	125	200	120	120
Averaging time (s)	0.6	0.09	0.06	0.1	0.1
Full scale equiv. averaging time (s)	0.6	0.6	0.6	1.22	1.6

been used. In general the model concentration histories were averaged over the standard full-scale averaging interval (0.6 s) but where the probe frequency response was inadequate at small scale, then the full scale data was smoothed accordingly (as Table 4). In the model experiments a large number of measurements (typically in excess of 100) were made to enable concentration contours to be drawn and comparison with full scale positions was made either directly or by contour interpolation.

3. Sample results

It is not the purpose of this paper to discuss detailed aspects of concentration fluctuations in time or in space across the measurement field but it is appropriate to display some sample results before presenting the data in a statistical form.

3.1 Time histories

Figure 4 shows an example of a Thorney Island concentration trace together with wind tunnel simulations at 1:40, 1:100, 1:150 and 1:250. The effect of probe frequency response has been removed by averaging all signals over blocks of 1.6 s. It can be observed that the smaller scales do indeed have noticeably less turbulent character as would be commensurate with increasing viscous damping at the smaller Reynolds numbers. Beyond that it would be unwise to conclude much from a snapshot of a single position in the field of a dispersing cloud. Examples have been given previously [4], for an instantaneous release, where qualitative comparisons showed quite different features for three positions in the same cloud. Apart from spatial effects in the same realisation, variability can also be seen between repeated simulations. Figure 5 shows an

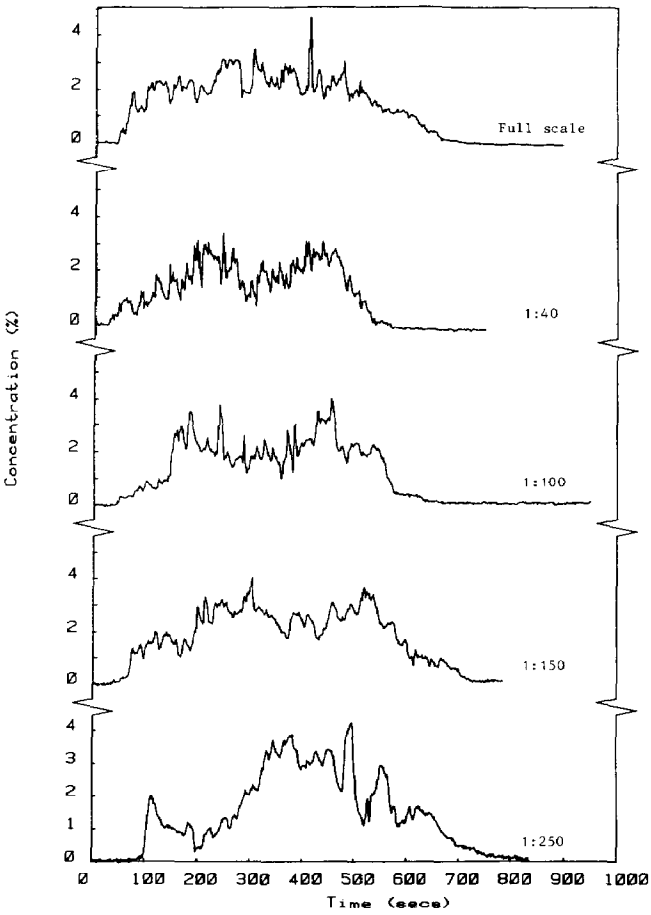

Fig. 4. Concentration time histories at model and full-scale (time base, full scale). Trial 037 ($X=9.4$ m, $Y=18.8$ m)

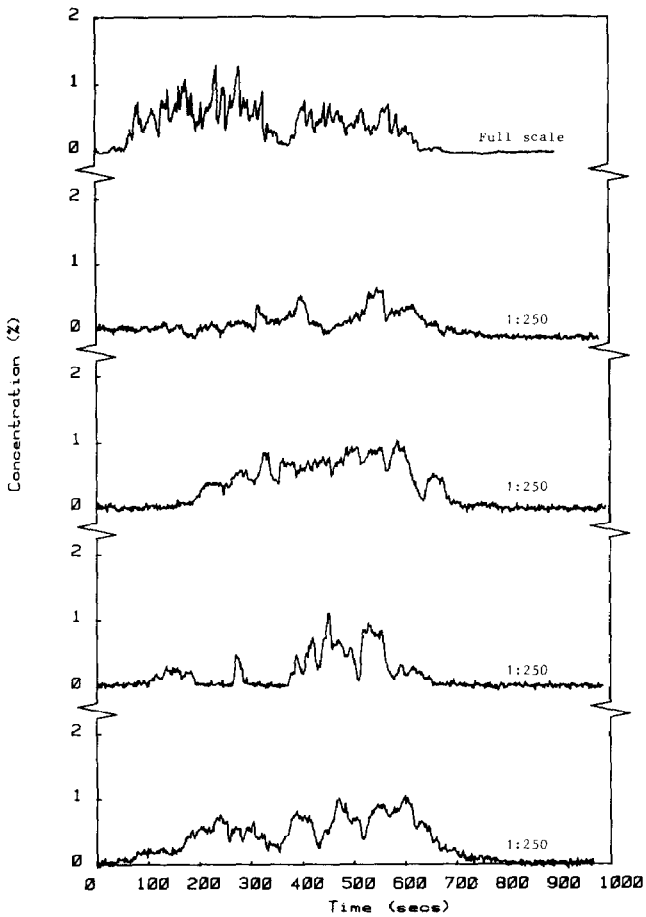

Fig. 5. Concentration time histories with four repeats at 1:250 scale (time base, full scale). Trial 037 ($X = -1.4$ m, $Y = 82.2$ m)

example of four repeats at 1:250 scale. The peak concentrations are low (Fig. 6 identifies a peak value of 1.25% at full scale at the mast position 82 m along the Y axis) and given the cloud direction, the measurement position was clearly close to the cloud edge. Under such circumstances it is not surprising that the detailed structure of the cloud (as described by the concentration history) is not well repeated.

3.2 Ground level peak concentration contours

Figure 6 illustrates a contour plot of peak levels averaged over an appropriate time (see Table 4). The contours derive from the wind tunnel simulation and the circled values represent the Thorney Island measurements at 0.4 m from the ground. Further examples of the data base of measurements are given in

Figs. 7 and 8, which contain the contour maps at all scales used for an instantaneous spill (Fig. 7, Trial 019) and a "continuous" release (Fig. 8, Trial 046). In subsequent discussion where point by point comparison statistics are referred to data will be drawn either from exact spatial simulations or from interpolations among the "model" contours at the full-scale location.

3.3 Centre-line concentration decay

A certain amount of automatic processing of the data was possible as can be seen in Fig. 9. Here the "centre-line" (points within 20 m of the wind axis) peak concentration data have been fitted with a polynomial and the 2% concentration downwind distance has been automatically computed and displayed. The data are for Trial 033 which was of Type 4.

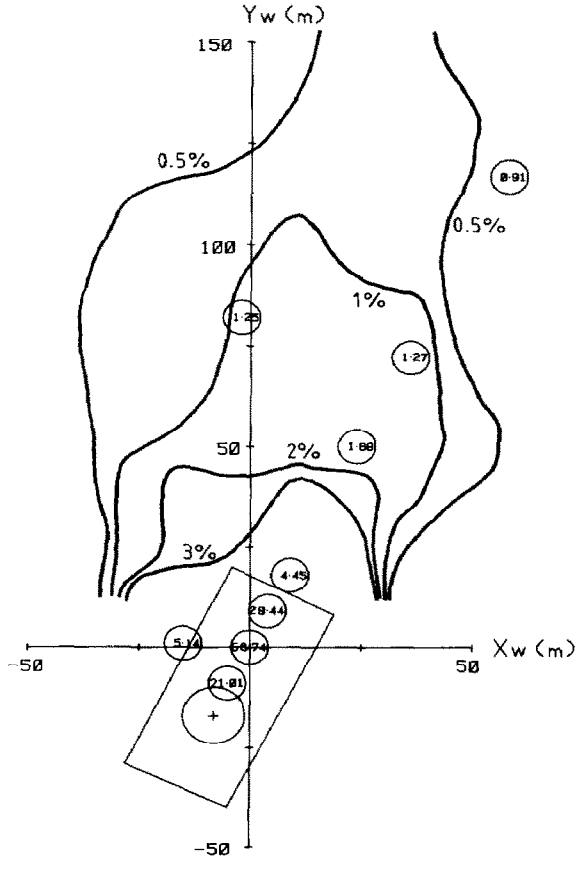

Fig. 6. Peak concentration contours for Trial 037 at 1 : 250 scale. Full-scale measurements encircled.

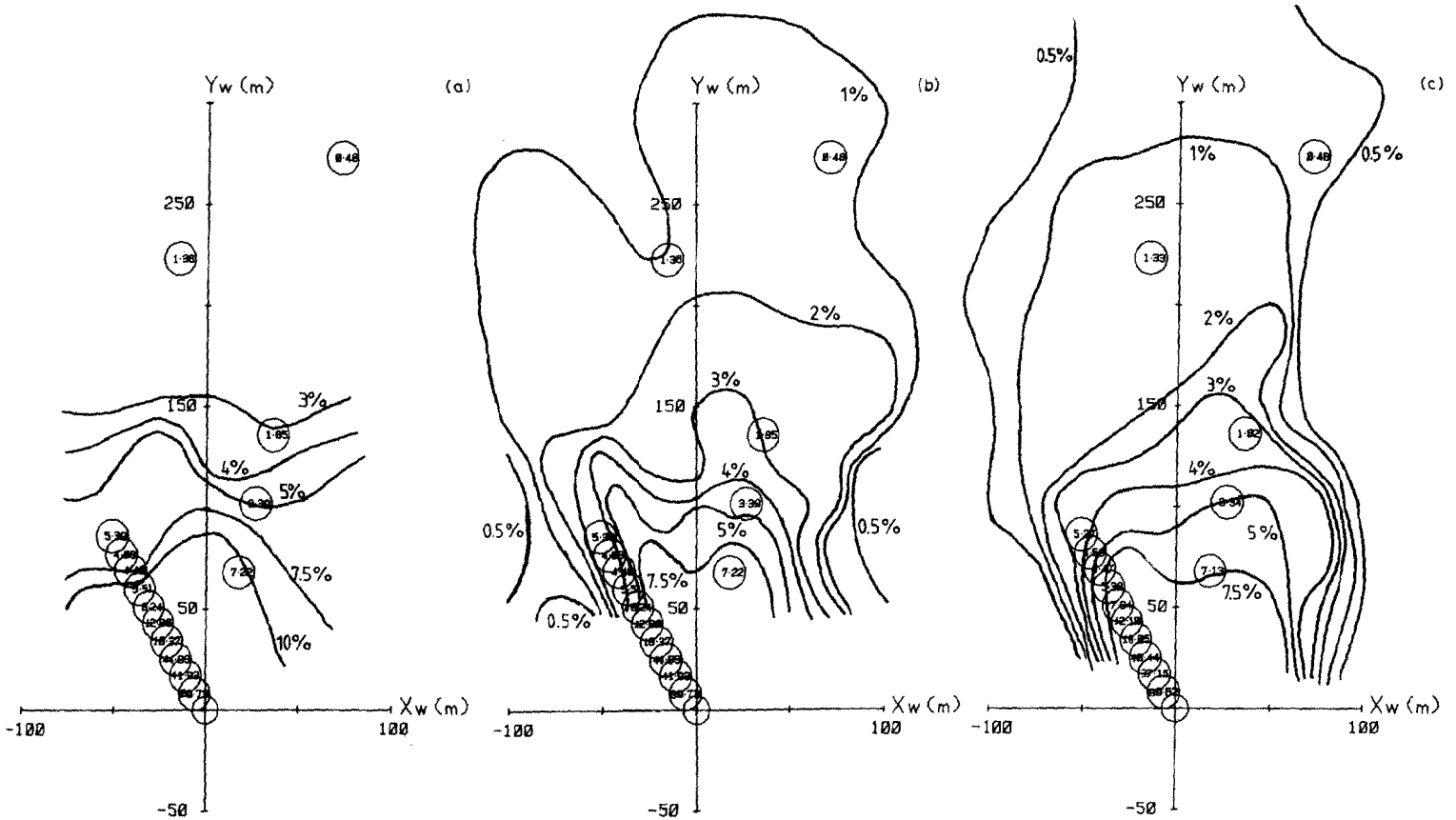

Fig. 7. Peak concentration contours for Trial 019: (a) 1:40, (b) 1:100, and (c) 1:150.

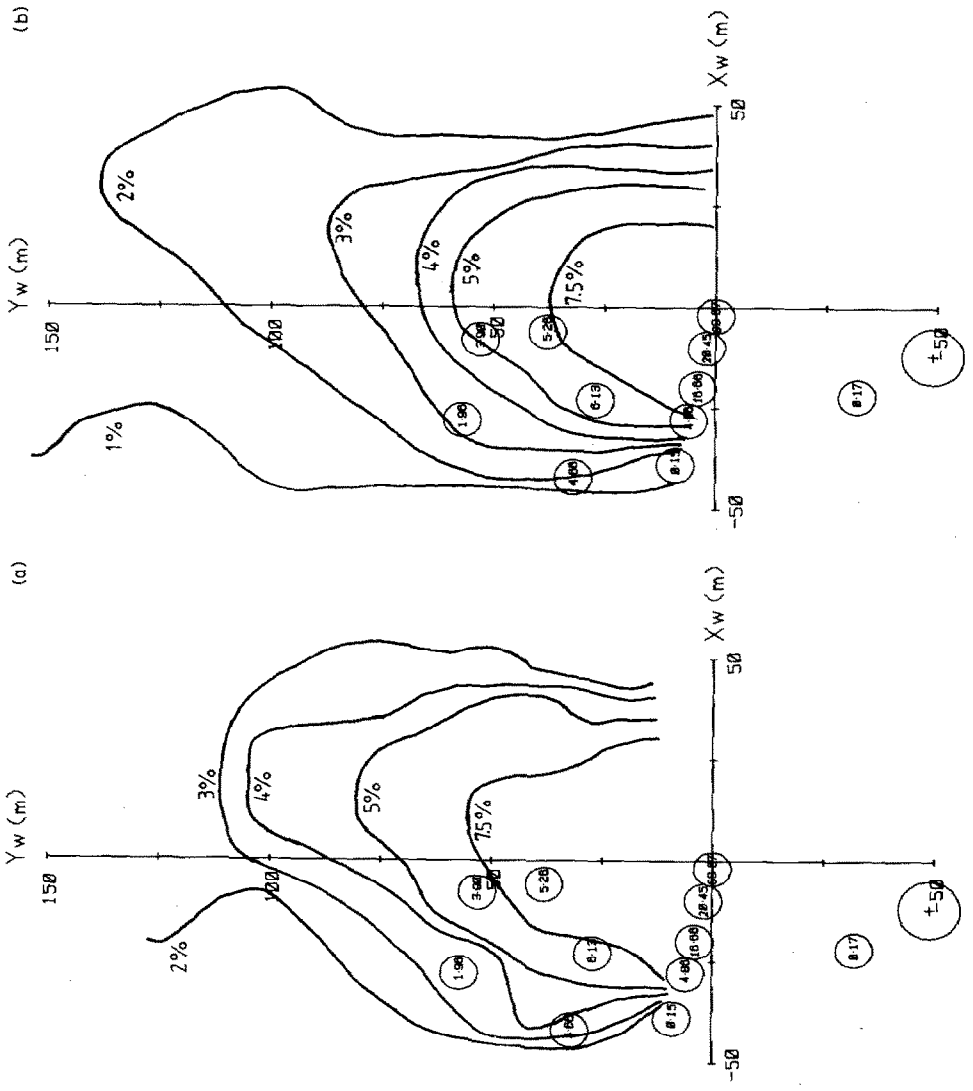
(b)
Yw (m)
Xw (m)
150
100
50
-50
1%
2%
3%
4%
5%
7.5%
±50
(a)
Yw (m)
Xw (m)
150
100
50
-50
2%
3%
4%
5%
7.5%
±50

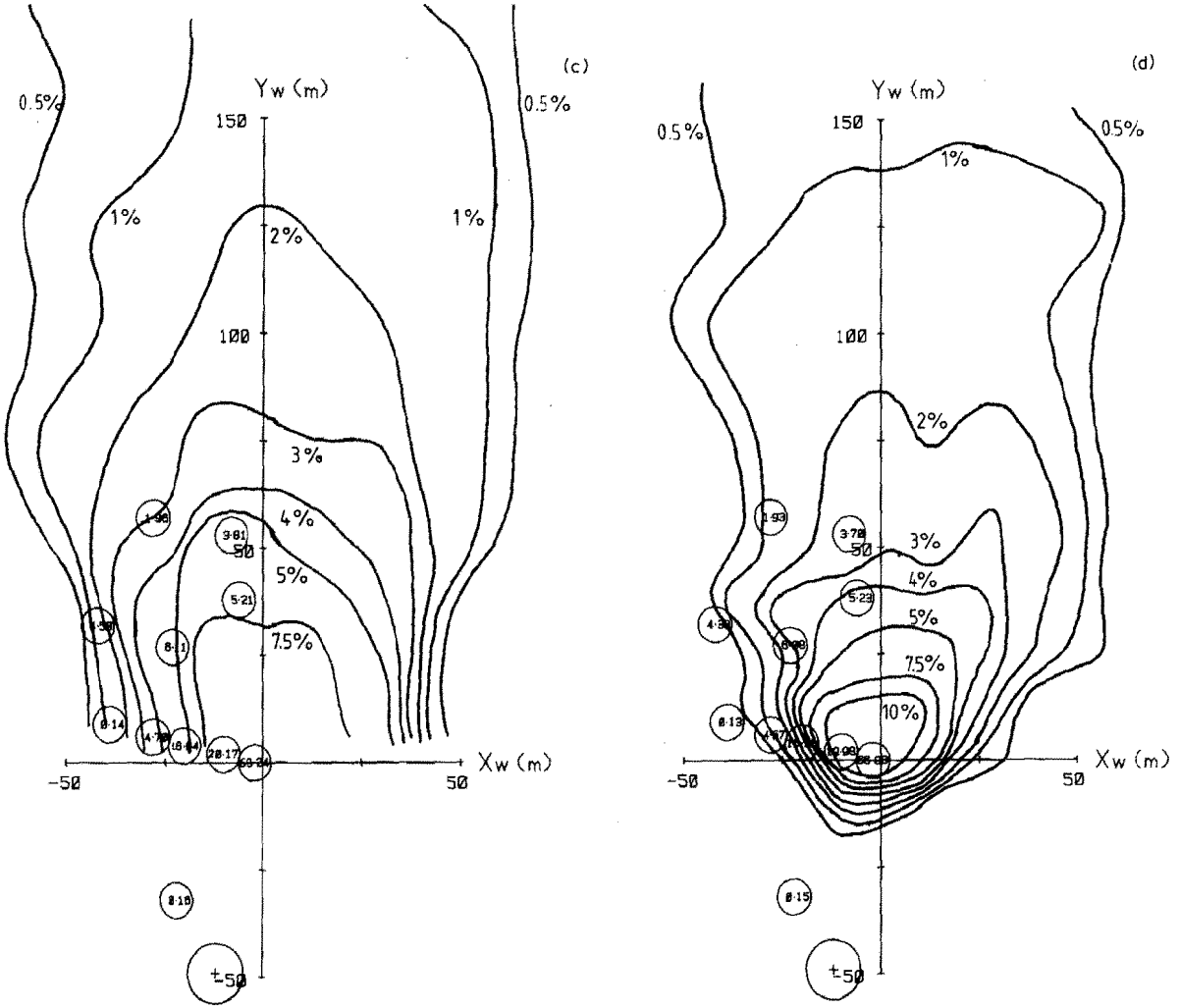

Fig. 8. Peak concentration for Trial 046: (a) 1:40, (b) 1:100, (c) 1:150, and (d) 1:250.

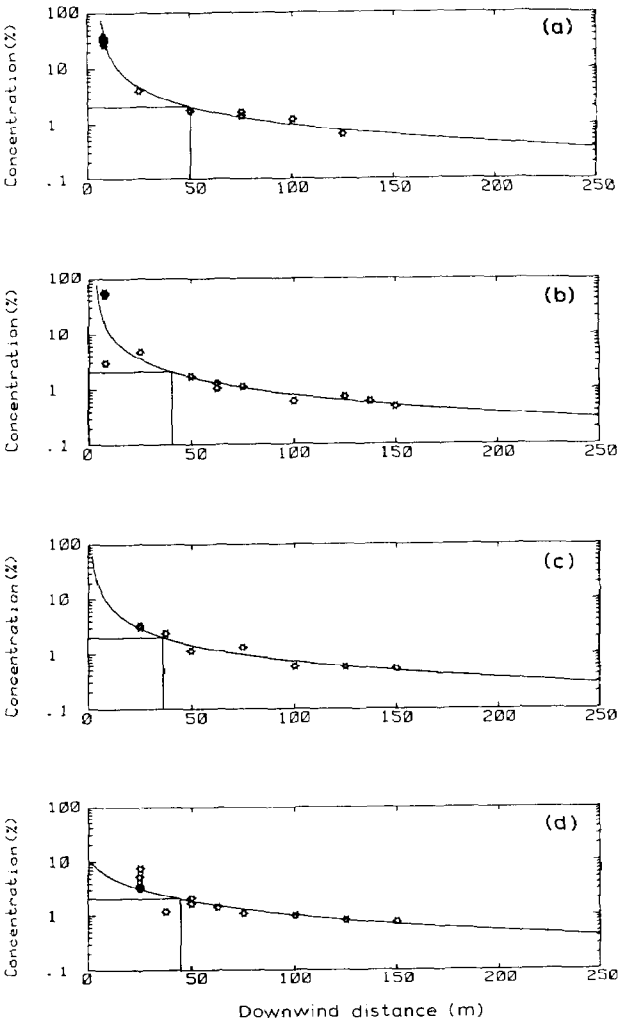

Fig. 9. Centre-line peak concentration decay at all scales (Trial 033): (a) 1:40, (b) 1:100, (c) 1:150, and (d) 1:250.

4. Statistics of model-full scale comparisons

The 86 simulations performed generated an order of magnitude greater number of potential point to point comparisons. The range of analyses is obviously large and the work to date has been confined to a study of a single statistic,

namely the peak concentration averaged over a time interval given in Table 4 and discussed in Section 2.

Perhaps the most obvious comparison is that shown in Fig. 10, where the peak model concentrations have been plotted against the full-scale values for the separate model scales used (in this case for all Phase III trials). Perfect correlation would produce a cluster of points on the 45° line. In practice the variability (both model and full-scale) produces a scatter within which a trend or limit of confidence must be determined (this is quantified in Figs. 11 and 12). Figure 10 differentiates between "exact" position replication in the sim-

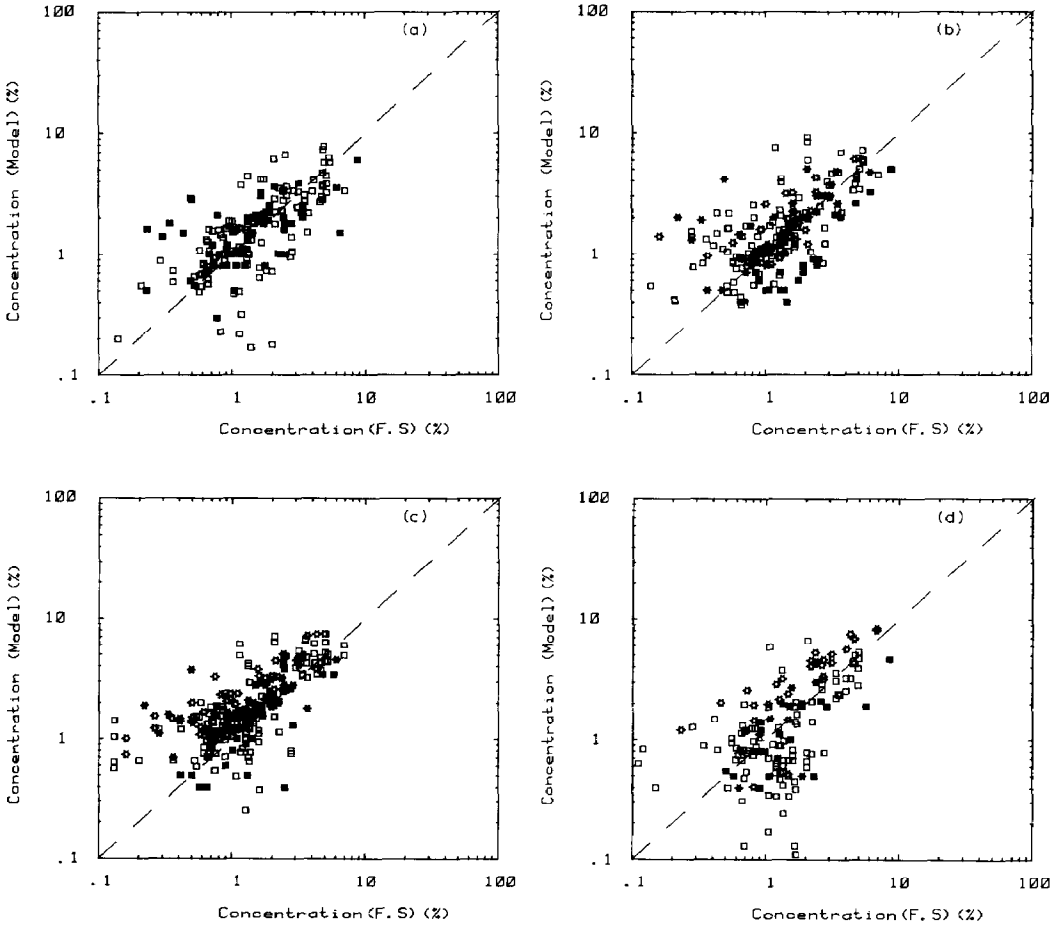

Fig. 10. Scatter plot of concentration at model scale against peak concentration at full scale. Phase III Thorney Island Trials: (a) scale 1:40, (b) scale 1:100, (c) scale 1:150, and (d) scale 1:250. Key: Open symbols: exact positions matched at model and full scale; Filled symbols: model results interpolated from contour plots; Squares: exact Froude scaling; and Stars: modified scaling.

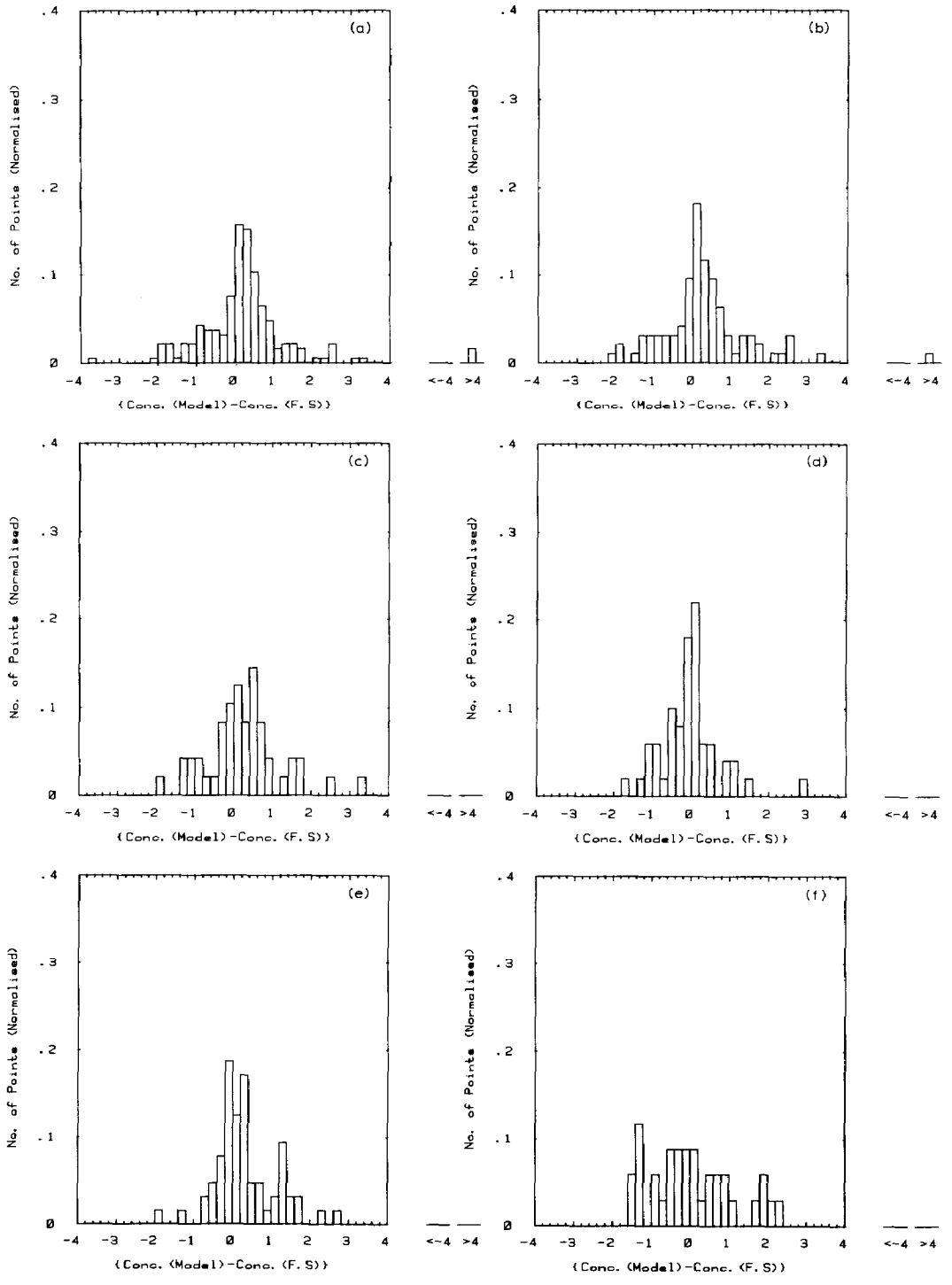
(a)
(b)
(c)
(d)
(e)
(f)
No. of Points (Normalised)
.4
.3
.2
.1
0
-4 -3 -2 -1 0 1 2 3 4
<-4 >4
(Conc. (Model)-Conc. (F. S))

ulations and interpolated data from contour maps. It can be argued that the interpolated data may yield more stable estimates but this is of little value when the trials data are a single realisation at a particular point only.

It is not evident that there is any particular trend in relation to modified Froude scaling or interpolated data. The general impression is one of slightly conservative model predictions (model/full-scale > 1) with a tendency toward less conservative estimates at 1:250 scale.

Frequently the absolute concentration is of more interest than a ratio of model to full-scale. This is particularly so in the determination of flammable boundaries or in estimates of the flammable inventory of a cloud. Figure 11 has, therefore, been constructed using the difference between peak (model) and peak (full-scale) as the measure of interest. Figure 11 shows a sequence of amplitude distributions where in (a), (b) and (c) the range of concentration values is gradually reduced to a region of specific interest around 2% (2% represents the equivalent of an LNG 5% LFL in an isothermal simulation) and (d), (e) and (f) complete the picture for the range of model scales used. The properties of the amplitude distributions are given in Table 5. The mean values are all positive with the exception of (d) (1:100 scale), but in fact the correlation in this case is the best of all ($\mu = -0.05\%$) and the scatter ($\sigma = 0.57\%$) is the smallest value computed. In contrast at 1:250 although the correlation is good on average ($\mu = 0.06\%$), the standard deviation is greater and Fig. 11(f) shows the flatness to be expected from the calculated kurtosis.

TABLE 5

Statistics of concentration difference for Type 4 spills.
$\Delta c = c$ (model) $- c$ (full scale), μ = mean of Δc distribution, σ = standard deviation, s = skewness, and k = kurtosis (flatness).

	Spill type	Scale	Concentration range (%)	Statistics of Δc (%)				No. of points in sample
				μ	σ	s	k	
(a)	4	1:40	0–100	0.22	1.57	+1.1	10.7	184
(b)	4	1:40	0–5	0.30	1.42	+1.9	11.8	94
(c)	4	1:40	1–3	0.25	0.91	+0.6	4.4	48
(d)	4	1:100	1–3	−0.05	0.57	+1.2	7.3	50
(e)	4	1:150	1–3	0.33	0.62	+0.4	4.3	64
(f)	4	1:250	1–3	0.06	1.14	+0.5	2.6	34

Fig. 11. Amplitude distributions for Δc (model − full-scale) for Type 4. (a) 1:40, no. of points 184, all sensor levels, concentration 0–100%; (b) 1:40, no. of points 94, sensor level 0.4 m, concentration 0–5%; (c) 1:40, no. of points 48, sensor level 0.4 m, concentration 1–3%; (d) 1:100, no. of points 50, sensor level 0.4 m, concentration 1–3%; (e) 1:150, no. of points 64, sensor level 0.4 m, concentration 1–3%; (f) 1:250, no. of points 34, sensor level 0.4 m, concentration 1–3%.

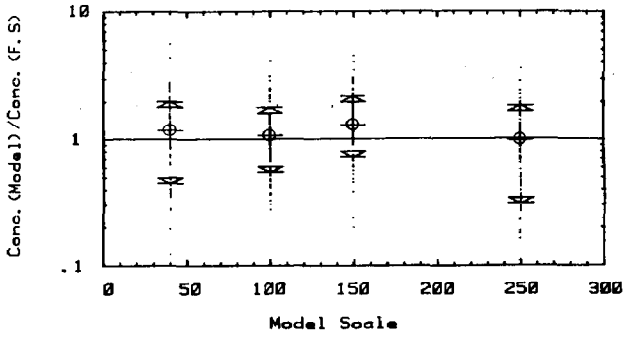

Fig. 12. Concentration scatter in decile bands: Type 4 trials, all sensor levels, concentration 0.5–3%, ⊖ median, △ and ▽ upper and lower deciles.

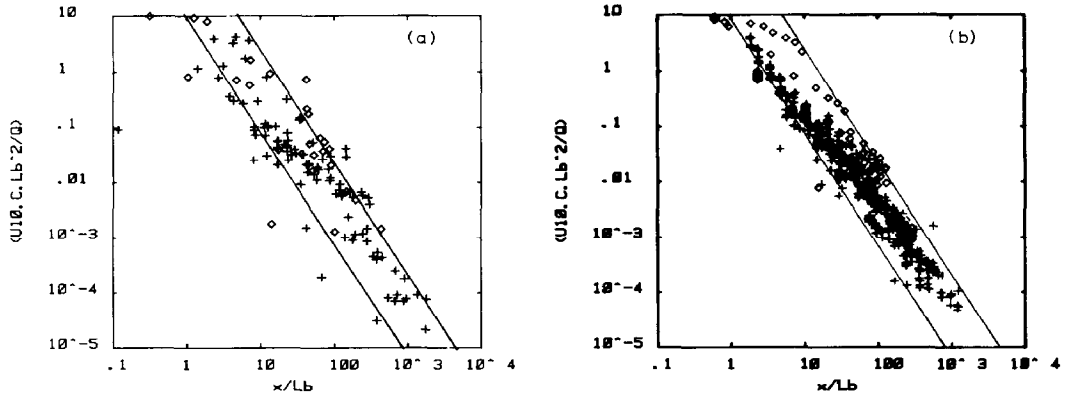

Fig. 13. Non-dimensional concentration decay with downwind distance – Types 3 (◇) and 4 (+) Trials. Solid lines represent limits of data in Meroney and Neff [5]. (a) Full scale, and (b) all simulation scales.

A composite picture of these results appears in Fig. 12, where the horizontal bar represents the mean ratio of model: full-scale and the outer marks show deciles of the respective distributions. Similar analyses for Types 1, 2 and 3 suggested the same trend of somewhat conservative average predictions becoming slightly less so with decreasing model scale.

The interest in wind tunnel model prediction is frequently not as general as all concentration levels at all points in the field. A convenient presentation of decay of peak concentration (c) with downwind distance (x) is given in non-dimensional form (e.g. by Meroney and Neff [5]) through, the reduced concentration $U_{10}cL_b^2/Q$, and the distance x/L_b, where the buoyancy length $L_b = g(\Delta\rho/\rho)(Q/U_{10}^3)$.

The data from the Type 3 and 4 trials are shown thus in Fig. 13. The collapse

is generally fair and the model to full scale comparison is encouraging. The solid lines represent the range of data plotted by Meroney and Neff [5], where the upper line is that referred to as the Battelle Columbus Laboratories Correlation in the reference. The Thorney Island full scale and simulation results fall consistently with this data. The limits drawn have a slope of -2 which exactly reduces the relationship to $c \sim (x/L_q)^{-2}$ ($L_q = (Q/U_{10})^{\frac{1}{2}}$) and removes any dependence on initial Richardson number. It was noticed that the Type 3 data showed evidence of a somewhat slower decay (especially at model scale) and that the data collapsed much better as c vs. x/L_q with Trial 038 (strongly influenced by the upwind gas container at -20 m) separating itself from Trials 045–047 (container to side or at least 50 m upwind). Whereas at model scale initial Richardson number insensitivity might arise because of an absence of

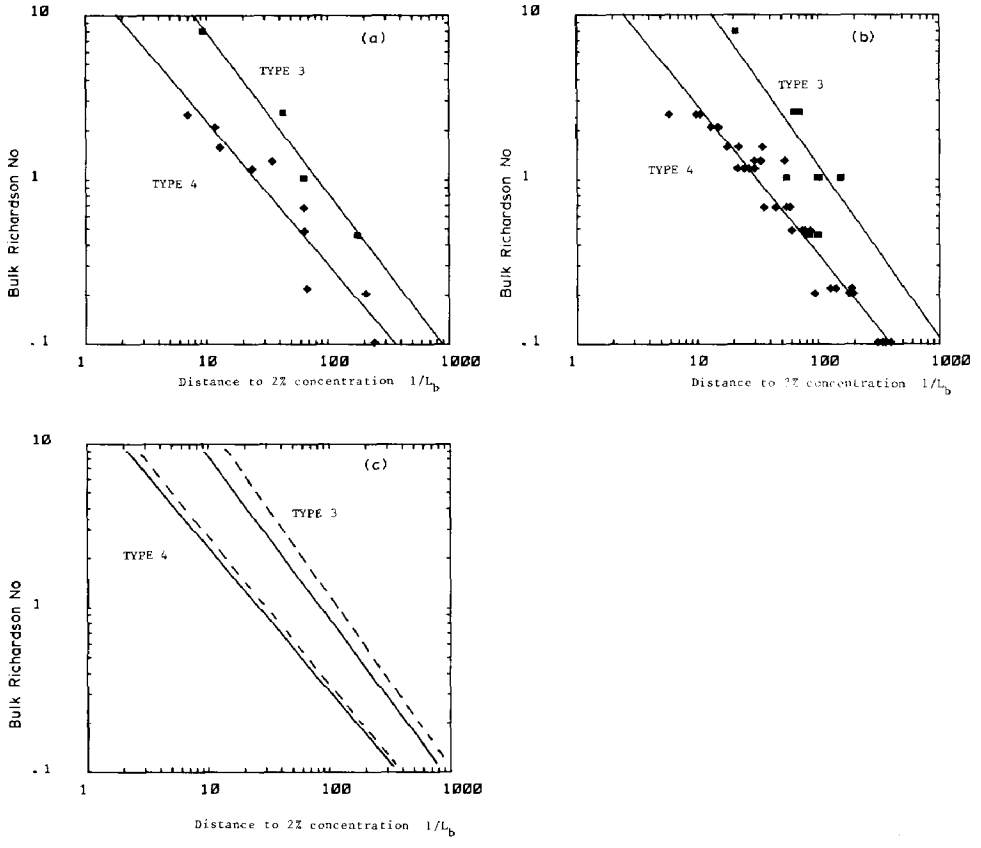

Fig. 14. Variation of distance to 2% concentration with bulk Richardson number. Type 3 (■) and 4 (◆) Trials. (a) Full scale data, (b) Simulation data at all scales, (c) Comparison of full-scale (——) and simulation data (— — —).

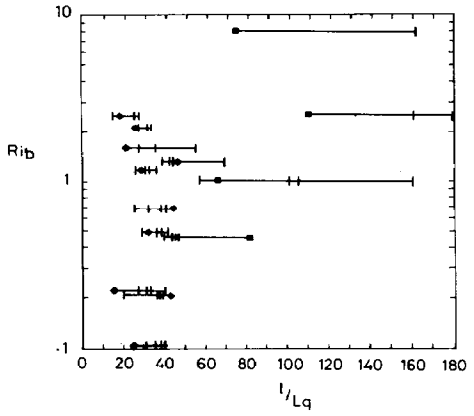

Fig. 15. Distances to 2%. Full scale: ■ Type 3, ◆ Type 4. Simulations: ++ (the horizontal line indicates the span of the simulation results, vertical lines denote individual simulations).

dense gas effects, the similar trends at full scale suggest a genuine physical explanation.

In order to compare dispersion distance prediction against source condition, the furthest distance to the 2% peak (l) is expressed as a function of initial bulk Richardson number (Ri_b) (Table 2) in Fig. 14. The bounded and unbounded spills are shown together to demonstrate the effect of the vapour fence in reducing dispersion distance. As can be seen the data are reasonably well represented by the best fit lines and the comparison in Fig. 14(c) indicates that in general the wind tunnel simulations give a slightly conservative absolute measure of downwind distance but slightly over predicted the change effected by the vapour fence. The slopes in Fig. 14 are close to unity, indicating a lack of dependence of l on Ri_b. This is seen to be substantially so in Fig. 15 where approximate straight vertical lines could be drawn through the Type 3 and 4 results. Clearly the linear axis exposes the variability more readily but it can be seen that (for Type 4 – with fence) the variability in the model results is not markedly different from that at full scale as judged by trials at similar Richardson numbers. (It was also noted that the figure differed little if $\Delta\rho/\rho$ were used on the ordinate rather than Ri_b.) The full-scale distances for Type 4 range from l/L_q of around 15 to 50 and whilst variability must account for some of the range, orientation of the enclosure to the wind (see Fig. 6) may also have played a part. The unbounded continuous spill data (Type 3) is relatively sparse and conclusions are difficult to draw, especially as in the lowest Ri_b case (Trial 038) the gas container was relatively close upwind. Taking, therefore, just the Phase I Type 3 results (see Table 2) the full scale range of l/L_q was about 2:1 (60 to 110) whereas the model results spanned 3:1 (60 to 180).

Surprisingly for the instantaneous data examined (Type 1, Fig. 16) there

also appeared to be little definite variation of l with Ri_b. The data set is rather small but to the extent to which an indication is given by the four trials simulated at more than one scale, the results all sit comfortably about the Thorney Island measurements.

So far the wind tunnel measurements have been characterised by the linear scale of the model. Clearly in terms of fundamental physical parameters this is unsatisfactory and recourse is sought in expressions of fluid dynamic scales.

It has been suggested by Puttock [6] that molecular rather than turbulence diffusion will predominate at ratios of $Pe/Ri_b > 1500$, where $Pe/Ri_b = U^3/g\,(\Delta\rho/\rho)\,D$ and U is a reference velocity, say U_{10} and D is the molecular diffusivity of the dispersing gas in air.

Taking all the data analysed in these experiments and comparing model

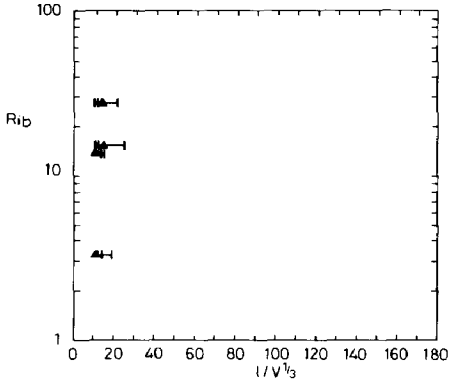

Fig. 16. Distances to 2% for Type 1. Full scale: ▲. Simulations: ++ (as Fig. 15).

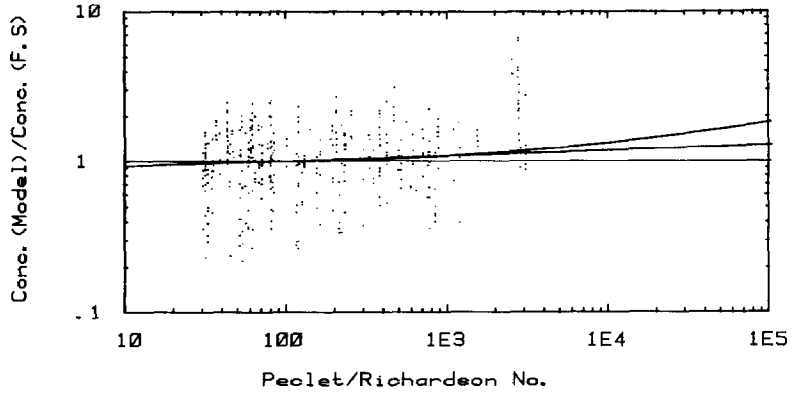

Fig. 17. Model/full scale concentration ratios as a function of Pe/Ri. All simulations for all phases for sensors at 0.4 m and concentrations between 0.5% and 3% (full scale). Linear and quadratic best fits drawn through data.

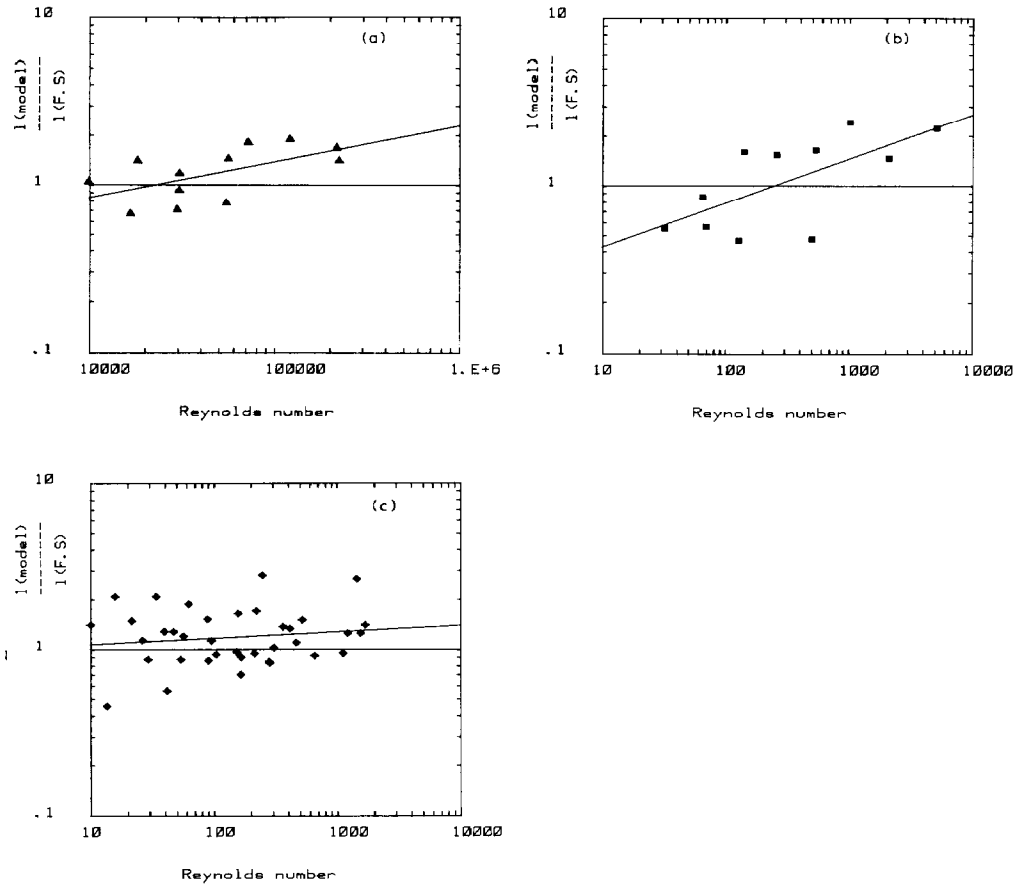

Fig. 18. Distance to 2% comparisons based on Re with buoyancy length scale ($Re = U_{10}L_b/\nu$) with least squares straight lines through all data: (a) Type 1, (b) Type 3, and (c) Type 4.

peak concentrations with full scale values on a point by point basis produces Fig. 17. No apparent trend can be discerned within the scatter and this is emphasised by the least squares straight line and quadratic which are drawn. The linear trend is slightly downward with reducing Pe/Ri_b crossing unity at around 100. However, an examination of the data in bands of Pe/Ri_b showed a level median at lower values and this is shown by the best fit quadratic which is fairly flat over much of the data range.

More particularly there is an attraction to return to the 2% dispersion distance for a compression of the data and finally in Fig. 18 this information is examined against the simulation Reynolds number with the buoyancy parameter L_b as the length scale; remembering that $L_b = Ri_b L_q$, where L_q is a length scale of the release $(Q/U_{10})^{\frac{1}{2}}$ for Types 3 and 4 and (volume)$^{\frac{1}{3}}$ for Types 1 and 2.

Once again establishing a significant statistical trend within the data is difficult, but some evidence of lower Reynolds number limits for safe (conservative) predictions begin to emerge especially when the dispersion is not influenced by sharp edged turbulence generators such as fences and buildings (i.e. Types 1 and 3, Figs. 18(a) and (b)). Rather clearer from Fig. 18(c) is the message that taking account of variability through the use of a suitable estimator applied to the available data may be more important than a slavish adherence to a particular model scale criterion. The line in Fig. 18(c) represents the best fit to the data. The slope is, however, strongly influenced by the extreme 10% of the points and without these the best-fit line has a reverse slope of similar magnitude. It should be concluded, therefore, that $l_{\text{model}}/l_{\text{full-scale}}$ is a weak function of scale (Re) with a mean value a little greater than unity. The variability in Fig. 18(c) suggests that to obtain with 90% confidence, a full scale prediction from a single estimate at model scale, the prediction should be placed in the band ($0.5\ l_{\text{model}}$, $2\ l_{\text{model}}$). Ideally, of course, the simulation would be run many times and the model-scale distribution of estimates established. The resulting probability statement could then be used as a more sophisticated prediction, though differentiating between genuine variability of the process (as at full scale) and simple model scale uncertainty remains an issue.

5. Conclusions

The Thorney Island data set has provided a rich source of information against which to validate wind tunnel modelling. The extent of possible analysis is far greater than has been covered in this paper, where essentially all comparisons and judgements have been made on peak concentration levels (suitably averaged). Within the scope of this work the wind tunnel simulations have emerged as an effective predictor of full-scale both from the qualitative phenomenological standpoint and with certain qualifications on the quantitative side. The major qualification concerns variability of the results. This occurs at model and full-scale and is believed to be an essential part of the physics rather than a manifestation of measurement inaccuracy. In this respect the use of peak values obviously does not help, but an alternative *simple* measure for non-steady-state signals which relates to flammable limits is not easy to identify.

The average trend from the wind tunnel simulations was generally of conservative predictions of the limits of the cloud with a slight tendency to reducing conservatism at smaller scales. No obvious validity threshold of Peclet/Richardson number ratio was observed in the data and for dispersion in the presence of sharp edged obstructions quite acceptable predictions were found down to the lowest Reynolds number utilised. For the unconfined "instantaneous" (Type 1) and "continuous" (Type 3) spills some evidence of lower Reynolds number limits have been produced.

It might be suggested that for Type 1, Re should be greater than about 23,000, where $Re = (U_{10}L_b/\nu)_{model}$ or $Re = (U_{10}Ri_b v^{\frac{1}{3}}/\nu)_{model}$, which equates to about a 1:120 scale modelling limit for a Thorney Island trial such as Trial 008. For a realistic full-scale hazard, smaller scales could be used due to the dependence on the total volume.

For Type 3 the limited data suggests a threshold between $Re = 100$ and 250, where L_b depends on the volume release rate. However this is largely dictated by one low Richardson number spill (four simulations of Trial 046) and thus depends on only one full scale measurement. Even so the resulting limit would not be particularly stringent, leading to a scale threshold of 1:170 to 1:300 for Trial 045.

6. Acknowledgements

The authors wish to thank the U.S. Gas Research Institute and the U.K. Dept. of Trade and Industry for their support for this work and for permission to publish the results.

References

1 J. McQuaid (Ed.), Heavy Gas Dispersion Trials at Thorney Island, (Chemical Engineering Monographs, 22) Elsevier, Amsterdam, 1985.

2 J. McQuaid and B. Roebuck, Large scale field trials on dense vapour dispersion, Report no. EUR 10029, Commission of the European Communities, Brussels, 1985.

3 M.E. Davies and S. Singh, Thorney Island: Its geography and meteorology, J. Hazardous Materials, 11 (1985) 91–124.

4 M.E. Davies, The validity of densimetric Froude number scaling in heavy gas studies, In: Proc. 2nd Workshop on Wind/Water Tunnel Dispersion Modelling, September 1984, Oxford, Report No. TPRD/L/2945/N85, Central Electricity Research Lab., Leatherhead, Surrey, 1984.

5 R.N. Meroney and D.E. Neff, Laboratory simulation of liquid natural gas vapor dispersion over land or water, In: J.E. Cermak (Ed.), Wind Engineering, Pergamon Press, 1980, pp. 1139–1150.

6 J.S. Puttock and G.W. Colenbrander, Dense gas dispersion — Experimental research, In: Proc. Heavy Gas (LNG/LPG) Workshop, January 29–30, 1985, Concord Scientific Corporation, Toronto, Canada.